with the cells of the larval salivary gland. Therefore, any specific conclusions applied to one class of somatic cells having restricted synthetic activities during an immature developmental stage. Pseudonurse cells, in contrast, are derived from the germ line, are present in the reproductive system of the adult female, and contain chromosomes that undergo a greater variety of morphological changes during their growth than do salivary gland chromosomes. Since all chromosome arms can be cytologically marked, the synthetic activities of specific chromosome segments can be contrasted at various developmental stages. The differential replication of euchromatin and heterochromatin and the relation between the relative amounts of chromosomal proteins and the coiling behaviors of these giant chromosomes are also targets for future investigations.

ROBERT C. KING*
SHAWN F. RILEY
JOSEPH D. CASSIDY
PEACHIE E. WHITE

Department of Biological Sciences, Northwestern University, Evanston, Illinois 60201

YONG K. PAIK

Department of Genetics, Hanyang University School of Medicine, Seoul 133, Korea

References and Notes

1. T. S. Painter, *Genetics* **19**, 175 (1933). For recent reviews see Lefevre (2) and Ashburner and Berendes (3).
2. G. Lefevre, in *Genetics and Biology of* Drosophila, M. Ashburner and E. Novitski, Eds. (Academic Press, London, 1976), vol. 1a, p. 31.
3. M. Ashburner and H. D. Berendes, in *ibid.*, M. Ashburner and T. R. F. Wright, Eds. (Academic Press, London, 1978), vol. 2b, p. 315.
4. M. Mariani and C. Bruno-Smiraglia, *Boll. Soc. Ent. Ital.* **87**, 23 (1957); M. Coluzzi, *Parassitologia* **10**, 179 (1968).
5. M. Coluzzi, G. Cancrini, M. DiDeco, *Parassitologia* **12**, 101 (1970); U. T. Saifuddin, R. H. Baker, R. K. Sakai, *Mosq. News* **38**, 233 (1978).
6. R. C. King, *Ovarian Development in* Drosophila melanogaster (Academic Press, New York, 1970), figure VI-1.
7. ——— and J. D. Mohler, in *Handbook of Genetics*, R. C. King, Ed. (Plenum, New York, 1975), vol. 3, p. 757.
8. R. C. King, R. G. Burnett, N. A. Staley, *Growth* **21**, 239 (1957).
9. R. C. King, E. A. Koch, G. Cassens, *ibid.* **25**, 45 (1961); R. C. King, J. H. Sang, C. B. Leth, *Exp. Cell Res.* **23**, 108 (1961).
10. M. Gans, C. Audit, M. Masson, *Genetics* **81**, 683 (1975).
11. R. C. King, M. Bahns, R. Horowitz, P. Larramendi, *Int. J. Insect Morphol. Embryol.* **7**, 359 (1978); C. K. Dabbs and R. C. King, *ibid.* **9**, 215 (1980).
12. B. Hochman, in *Genetics and Biology of* Drosophila, M. Ashburner and E. Novitski, Eds. (Academic Press, London, 1976), vol. 1b, p. 903.
13. J. Schultz, *Brookhaven Symp. Biol.* **18**, 116 (1965).
14. W. Beermann, *Chromosoma* **5**, 139 (1952); in *Developmental Studies on Giant Chromosomes*, W. Beermann, Ed. (Springer-Verlag, New York, 1972), p. 1.
15. D. Ribbert, *Chromosoma* **74**, 269 (1979).
16. P. K. Mulligan and E. M. Rasch, in preparation.
17. E. M. Rasch, R. C. King, J. D. Cassidy, unpublished data.
18. R. C. King, in *Handbook of Genetics*, R. C. King, Ed. (Plenum, New York, 1975), vol. 3, figure 1, opposite p. 628.
19. We are grateful to Dr. Madeleine Gans for supplying the initial cultures of *fs(1)231* and *116* and to Dr. George Lefevre for the *Df(1)C159* stock. Drs. Eun Ho Park, Michael R. Cummings, Ralph M. Sinibaldi, Ellen M. Rasch, and James B. Kitzmiller gave useful suggestions.
This research was supported by National Science Foundation grant PCM7907597 and with funds from Lyun Joon Kim, former president of Hanyang University.
* Correspondence should be addressed to R.C.K.

1 August 1980; revised 15 December 1980

Adenosine 3′,5′-Monophosphate Waves in *Dictyostelium discoideum*: A Demonstration by Isotope Dilution–Fluorography

Abstract. *The distribution of adenosine 3′,5′-monophosphate (cyclic AMP) in fields of aggregating amoebae of* Dictyostelium discoideum *was examined by a novel isotope dilution–fluorographic technique. Cellular cyclic AMP was visualized by its competition with exogenous ^{3}H-labeled cyclic AMP for high-affinity binding sites on protein kinase immobilized on a Millipore filter used to blot the monolayer. The cyclic AMP was distributed in spiral or concentric circular wave patterns which centered on the foci of the aggregations. These patterns were correlated with those of cell shape change that propagate through the monolayers: cells in regions of high concentrations of cyclic AMP were elongated (presumably moving up a cyclic AMP gradient), whereas those in regions of low cyclic AMP concentrations were randomly directed. The highest cyclic AMP concentrations were about 10^{-6} M. The widths of the regions of elevated cyclic AMP were about 0.3 to 1 millimeter which, assuming a wave velocity of 300 micrometers per minute, suggests that a cell signals for about 1 to 3 minutes. These observations support the hypothesis that the aggregation process in* Dictyostelium *is mediated by the periodic relay of cyclic AMP signals and suggest a simple scheme for the dynamics of the aggregation process.*

Although it is clear that cells must communicate during morphogenesis little is known about how they do so. The cellular slime mold *Dictyostelium discoideum* can be used to examine this question. During one phase of its life cycle, separated amoebae begin to communicate and aggregate to form a multicellular structure which later undergoes a series of shape changes (*1–5*). Monolayers of cells on agar become segregated into territories; cells within each territory are attracted to its center. Early in aggregation, cells move in steps, advancing for about 2 minutes and then stopping for about 5 minutes before moving again (*6, 7*). Moving cells are elongated, and in dark-field photographs appear lighter than stationary, rounded cells (*7*). Light bands (moving cells) form spiral or concentric circular patterns about a center (see Fig. 1). In time-lapse films, each light band can be seen spreading outwardly from a center as an enlarging ring as cells progressively farther from the center begin an inward movement step (*8*). It has been proposed that the chemotactic movement steps are coordinated by extracellular signals of adenosine 3′,5′-monophosphate (cyclic AMP) which are propagated outwardly from the center (*9*). In this scheme, a cell

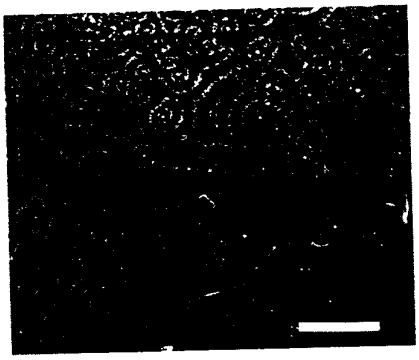

Fig. 1. Organized waves of cell movement during aggregation in *D. discoideum*. Techniques for growth and development of NC-4 amoebae closely followed those of Alcantara and Monk (*7*). "Starvation plates" were prepared just before use by pouring 9 ml of an autoclaved solution of 10 g of agar (Difco), 1.00 g of K_2HPO_4, 2.31 g of $KHPO_4$, and 0.5 g of $MGSO_4$ per liter into 100-mm petri dishes (Falcon 1001). Amoebae, grown in association with *Enterobacter aerogenes*, were freed of bacteria, and 1 ml of a cell suspension at a density of 8×10^7 cells per milliliter was added to each plate. The cell suspension was spread evenly by shaking the dish, and the cells were allowed to settle for 20 minutes. Excess fluid was removed and the lid was left off the dish for an additional 20 minutes or until a thin layer of surface fluid remained. The cultures were incubated at 7°C for 18 hours. Although the patterns shown were usually visible when the cultures were removed from the incubator, removal of the lid for about 15 to 20 minutes enhanced their appearance. Illumination was provided by a dark-field condensing lens system as described by Gross *et al.* (*8*). Calibration bar, 1 cm.

0036-8075/81/0424-0443$00.50/0

responds in two ways to cyclic AMP: it relays the signal by releasing additional cyclic AMP, and it moves in the direction from which the signal approaches. It has been shown that isolated amoebae can move up cyclic AMP gradients and release cyclic AMP in response to cyclic AMP stimuli (*10–12*). The hypothesis that the relay of cyclic AMP signals occurs during chemotactic aggregation on a surface is reasonable; however, the proposed waves of cyclic AMP have never been observed.

We now report direct visualization of the distribution of cyclic AMP in a monolayer of aggregating amoebae. The distribution of cyclic AMP was determined by using a competitive binding assay modified to occur on a surface as described below. Two Millipore filters were sequentially layered onto a monolayer. Cyclic AMP was drawn from the cells into the lower filter which contained ^{3}H-labeled cyclic AMP. Within 1 minute, a second filter, with protein kinase uniformly adsorbed to it, was placed on the first, and the cyclic AMP drawn into it bound to the protein kinase. The upper filter was washed extensively to remove unbound cyclic AMP, and then the bound labeled cyclic AMP was detected by fluorography. In this procedure the cyclic AMP extracted from the cells mixes with ^{3}H-labeled cyclic AMP in the lower filter, reducing its specific activity and, therefore, the amount of labeled cyclic AMP bound by the kinase on the upper filter. The regions of the monolayer containing high cyclic AMP concentrations significantly decrease the specific activity of the labeled cyclic AMP and appear as light areas on a dark background in the fluorograph (or as dark areas on a light background in a print of the fluorograph).

Fig. 2. Fluorographic image of cyclic AMP waves. Amoebae were developed to an early aggregation stage as described in Fig. 1. A Millipore filter (HA type, 0.45 μm, 9.0 cm in diameter) was soaked in 10 percent acetic acid containing 2.5×10^{-8} *M* ^{3}H-labeled cyclic AMP (New England Nuclear; specific activity 37 Ci/mmole), blotted to remove excess fluid, and gently layered onto the cell monolayer. After 1 minute the culture was moved to a 4°C room where the following steps were carried out. A second filter, which had previously been soaked in a solution of protein kinase (1 mg/ml), rinsed in 100 m*M* sodium acetate, *p*H 7, blotted, and set aside for several minutes, was layered onto the first. [Protein kinase was prepared from bovine heart (*34*); there was a total of 0.4×10^{11} cyclic AMP binding sites per square centimeter of the Millipore filter.] After 4 minutes, the upper filter was removed, washed three times for 5 minutes each time in separate 120-ml volumes of 17 m*M* potassium phosphate buffer, *p*H 6.2. The filter was blotted and left to dry at room temperature. When completely dried, it was dipped in a solution containing 7 g of 2,5-diphenyloxazole (New England Nuclear) per 100 ml of toluene, then dried again. The filter was placed between two clear plastic sheets and the side of the filter which had been against the lower filter was pressed against x-ray film (Kodak X-Omat R, XR-5) for 22 days at −70°C. The film was developed for 5 minutes in D19 (Kodak), fixed for 2 minutes, washed extensively with running water, and dried. The fluorograph was used as a negative to make this print. Calibration bar, 1 cm. (Completely black circles are artifacts caused by air bubbles trapped between the two filters.)

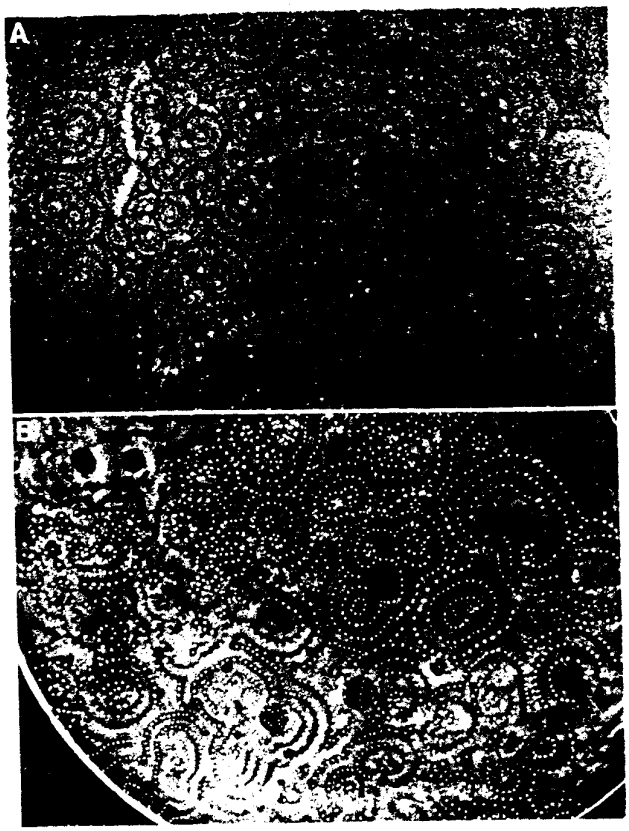

Fig. 3. Relative positions of moving and signaling cells. (A) Dark-field photograph of a section of the monolayer which produced the fluorograph shown in Fig. 2. (B) The thin black lines in (A) were traced by a series of dots onto a sheet of clear plastic. The fluorograph was used as negative and aligned with the tracing to make this print.

The pattern of cyclic AMP distribution in a monolayer of aggregating amoebae revealed by fluorography resembled the patterns of cell morphology seen in dark-field photographs. Figure 2 shows that the dark bands (high concentrations of cyclic AMP) form spiral or concentric circular patterns on a lighter background. Bands intersect but do not cross; overlapping arcs were not observed. Rather, V-shaped structures face each other at the two points of intersection of the arcs. The widths of the bands ranged from 0.3 to 1 mm and the distances between their centers varied from 0.5 to 2 mm. Both the width of the bands and the interband spacing increased with distance from the center of the territory.

We established that differences in optical density in the fluorographs reflect differences in cyclic AMP concentration within the cell monolayer. First, treatment of regions of the monolayer for 5 minutes with 1 m*M* NaN_3 [an inhibitor of cyclic AMP synthesis (*13*)] eliminated bands from those regions of the fluorograph. Second, fluorographs of unwashed upper filters did not show bands, indicating that ^{3}H-labeled cyclic AMP was transferred uniformly from the lower to the upper filter. Therefore, the patterns observed in washed filters must represent differences in the amount of labeled cyclic AMP bound to protein kinase. Third, bands were not detected

when the concentration of labeled cyclic AMP in the lower filter was increased to $5 \times 10^{-7}M$. Presumably, not enough cyclic AMP is drawn from the cells to significantly dilute the specific activity of this higher concentration. Fourth, 1-mm spots of $4 \times 10^{-7}M$ to $2 \times 10^{-7}M$ cyclic AMP applied to an agar surface produced nearly superimposable spots on the fluorographs (*14*).

The fluorographs were used to estimate the duration of an amoeba's signaling response in situ (*15–20*). A band represents an area of increased cyclic AMP concentration, that is, "signaling" cells (*13, 21*). The width of the band is the distance the wave travels during the time a cell is signaling. These widths vary from 0.3 to 1.0 mm, suggesting that the signal duration can vary. The velocity of the cyclic AMP waves is the same as that of the bands in dark-field photographs, about 300 μm per minute (*6, 7, 22*), indicating a range in signal duration from about 1 to 3.3 minutes [see (*14*)].

To determine the timing of a cell's movement and signaling responses, we compared fluorographs and dark-field photographs of the same region of monolayer (compare A and B in Fig. 3) (*23–26*). In dark-field photographs, a thin black line is apparent at the distal edge of the light bands (see Figs. 1 and 3A). A tracing of these lines was superimposed on the corresponding fluorograph. They aligned just distally to the bands of increased cyclic AMP (Fig. 3B). This indicates that the amoebae begin to move and signal at approximately the same time and that for a period they do both simultaneously. It was difficult to determine which response ceases first because the proximal edges of the light bands in the photographs were not clearly discernible.

The fluorographic images prove that there are cyclic AMP waves in the cell monolayer, give detailed information on their dimensions and concentration range, and indicate the relative position of the moving and signaling cells. Taken together with observations of the signaling response in vitro this information suggests a simple scheme for the dynamics of cyclic AMP signal relay and chemotaxis (see Fig. 4). We propose that the leading edge of the cyclic AMP wave is the gradient that orients a cell during a chemotactic movement step [see (*27, 28*) for quantitation of the cyclic AMP gradient]. As the cyclic AMP wave advances its mean extracellular concentration increases and the cell's rate of cyclic AMP secretion increases. Nevertheless, the cell remains in a gradient because cells closer to the peak are secreting at still higher rates. After several minutes, the peak of the cyclic AMP wave reaches the cell and it ceases its chemotactic movement step. [Since the cyclic AMP waves revealed by fluorography are quite symmetric, it is puzzling why a cell does not reorient (away from the center) as the wave passes (*29*).] In this scheme the duration of a movement step is determined not by internal cellular parameters but rather by the width and velocity of the cyclic AMP waves (*30*). The width, and perhaps velocity, of the waves are probably determined by the kinetics of the cyclic AMP signaling response. When cells are stimulated in vitro with cyclic AMP the rate of cyclic AMP secretion accelerates for about 2 to 3 minutes and gradually declines to basal levels (*20*). These kinetics of cyclic AMP synthesis are entirely consistent with the shapes of the waves we detected in situ.

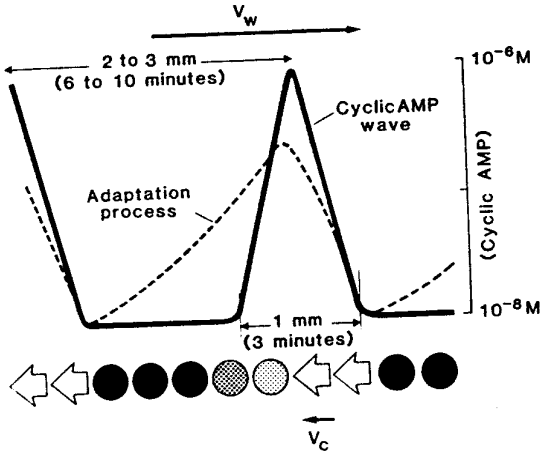

Fig. 4. Dynamics of signal relay and chemotaxis. The heavy line representing the cyclic AMP concentration is drawn from analyses of scans of the optical density of fluorographic images of the cyclic AMP waves [Fig. 2; see (*27*)]. The concentrations given are for total cyclic AMP detected in our measurements; extracellular concentrations may be considerably lower [see (*13, 21*)]. Symbols in lower part of diagram represent a single radial line of cells. Each would represent about 50 cells at a density of 10^6 per square centimeter. Large arrows represent chemotactically oriented cells while circles represent randomly oriented cells. (These symbols are shown as open or closed to correspond with the light bands and dark background seen in dark-field photographs. Two shaded circles indicate that the proximal edge in the dark-field photographs was not always clearly discernible.) Arrow vectors indicate the speed and direction of motion of the cyclic AMP wave ($V_w \cong 300$ μm/min) and the moving cells ($V_c \cong 20$ μm/min).

The transient nature of the cyclic AMP signaling response has been understood in terms of an adaptation process (*31*). The adaptation process has been sketched into Fig. 4. Cells on the proximal edge of the wave remain adapted for a time after cyclic AMP has been lowered. This explains why no overlapping arcs are observed in the fluorographs (Fig. 2). When wave fronts meet, adapted cells are encountered on each side of the boundary and consequently neither wave can be propagated. Gradually the adaptation process decays and the cells resensitize in time to respond to the next wave.

The technique of isotope dilution–fluorography provides a link between biochemical studies on isolated amoebae of *Dictyostelium* and observations of their behavior during aggregation. Furthermore, it should be generally applicable to culture monolayers, mutant colony selection, or even tissue slices, given the availability of binding proteins of high affinity and specificity (such as antibodies) directed against cellular or secreted biomolecules of interest.

K. J. Tomchik
P. N. Devreotes*
Department of Biochemistry, University of Chicago, Chicago, Illinois 60637

References and Notes

1. J. T. Bonner, *The Cellular Slime Molds* (Princeton Univ. Press, Princeton, N.J., 1961).
2. G. Gerisch, *Curr. Top. Dev. Biol.* 3, 157 (1968).
3. W. F. Loomis, *Dictyostelium Discoideum: A Developmental System* (Academic Press, New York, 1975).
4. P. C. Newell, in *Receptors and Recognition*, series B, vol. 3, *Microbial Interactions*, J. L. Reissig, Ed. (Chapman and Hall, London, 1978), p. 157.
5. M. Sussman and J. Schindler, *Differentiation* **10**, 1 (1978).
6. S. A. Mackay, thesis, University of Chicago (1979).
7. F. Alcantara and M. Monk, *J. Gen. Microbiol.* **85**, 321 (1974).
8. J. D. Gross, M. J. Peacy, D. J. Trevan, *J. Cell Sci.* **22**, 645 (1976).
9. B. Shaffer, *Adv. Morphog.* **2**, 109 (1962).
10. T. M. Konijn, D. S. Barkley, Y. Y. Chang, J. T. Bonner, *J. Bacteriol.* **99**, 510 (1969).
11. B. Shaffer, *Nature (London)* **255**, 549 (1975).
12. W. Ross, V. Nanjundiah, D. Malchow, G. Gerisch, *FEBS Lett.* **53**, 139 (1975).
13. M. C. Dinauer, S. A. Mackay, P. N. Devreotes, *J. Cell Biol.*, in press.
14. The mean ratio of the diameter of the spots detected by fluorography to that of the corresponding applied cyclic AMP spots was 1.11 (standard deviation = 0.07). This control indicates that the widths of the wider bands we observed (the majority) are reasonably accurate; however, we cannot rule out the possibility that some of the narrowest profiles observed (~ 0.3 mm) were not derived from very narrow (perhaps 0.1 mm) cyclic AMP distributions in the monolayer.
15. There is considerable controversy on this point. Cohen and Robertson (*16*) originally proposed a short signal duration (actually a delta function) to facilitate a mathematical treatment of aggregation [see (*4, 7*)]. Recently, Grutch and Robertson (*17*) reported a study of cyclic AMP signaling in which all the responses were brief (less than 20 seconds). Shaffer (*11*) and Ross *et al.* (*12*) were the first to measure the signal duration in vitro

and found it to be at least several minutes in duration. Other investigators have confirmed this result experimentally (*18*). Parnas and Segal (*19*) showed that it was theoretically possible for a signal of long duration to propagate. The results of Devreotes and Steck (*20*) indicate that the duration of the response depends on that of the stimulus but it can never be longer than several minutes. This suggests that a range of signaling durations might be observed in situ, the longest being several minutes.

16. M. Cohen and A. Robertson, *J. Theor. Biol.* **31**, 101 (1971).
17. J. F. Grutch and A. Robertson, *Dev. Biol.* **66**, 285 (1978).
18. J. S. Geller and M. Brenner, *J. Cell. Physiol.* **97**, 413 (1978).
19. H. Parnas and L. Segal, *J. Theor. Biol.* **71**, 185 (1978).
20. P. N. Devreotes and T. L. Steck, *J. Cell Biol.* **80**, 300 (1979).
21. G. Gerisch and V. Wick, *Biochem. Biophys. Res. Commun.* **65**, 364 (1975).
22. K. J. Tomchik and P. N. Devreotes, unpublished data.
23. There are several models of the temporal relation between the chemotactic movement and signal relay responses. Shaffer (*9*) first proposed that amoebae begin to signal after completing an inward movement step. Other authors have adopted this logical sequence of events (*24*). Cohen and Robertson (*16*) inverted the sequence suggesting that a cell emits a brief cyclic AMP signal about 15 seconds after receiving one and then begins the movement step. This hypothesis has gained acceptance (*4*, *7*) and computer simulations employing this hypothesis lead effectively to aggregation (*25*, *26*).
24. G. Gerisch, D. Hulser, D. Malchow, V. Wick, *Philos. Trans. R. Soc. London Ser. B* **272**, 181 (1975).
25. S. Mackay, *J. Cell Sci.* **33**, 1 (1978).
26. H. Parnas and L. A. Segal, *ibid.* **25**, 191 (1977).
27. A plot of the optical density of the fluorograph along the radius of a territory has the contour of a symmetrical wave with at least threefold differences in intensity. We estimated the concentration of the cyclic AMP bands by applying small drops of cyclic AMP directly to the monolayer just before assay. The bands were lighter than the spots produced by drops of $4 \times 10^{-7} M$ cyclic AMP but not as light as those produced by drops of $2 \times 10^{-6} M$. We also conducted control experiments on agar without cells by mixing unlabeled cyclic AMP of known concentration with the ^{3}H-labeled cyclic AMP in the lower filter. The cyclic AMP extracted from cells produced concentrations in the lower filter ranging from $10^{-8} M$ in the interpeak regions to $2 \times 10^{-7} M$ at the peaks. Assuming that extracellular cyclic AMP is a significant fraction of total cyclic AMP (detected in our measurements), the gradients encountered by cells in situ may be as steep as $10^{-6} M$ per millimeter. This is about 50-fold greater than reported threshold values (*28*).
28. J. Mato, A. Losada, V. Nanjundiak, T. Konijn, *Proc. Natl. Acad. Sci. U.S.A.* **72**, 4991 (1975).
29. Perhaps the adaptation process (see text) is linked to chemotaxis as well as cyclic AMP signal relay. Cells on the proximal edge of the cyclic AMP wave may be unable to sense the reversed gradient because they are relatively more adapted than those on the distal edge.
30. The duration of movement step is about 100 seconds (*7*, *16*). This is consistent with the dimensions of the cyclic AMP waves revealed by isotope dilution-fluorography. The width of half of the wave (about 0.5 mm) corresponds to a duration of about 90 seconds. A careful examination of movement step durations has revealed a considerable range (60 to 160 seconds) with the mean at 100 seconds (*6*). We predict that the different durations will correlate with differences in the width and velocity of different cyclic AMP waves.
31. A study of the kinetics of the adaptation process yielded detailed information on the increase in cyclic AMP upon introduction of a cyclic AMP stimulus (*32*) and its decrease upon stimulus removal (*33*). This knowledge has been used to sketch the level of the adaptation process within cells in the monolayer. For example, the decay of adaptation occurs with a half-time of about 3 or 4 minutes. In situ, the cyclic AMP wave would advance 0.9 to 1.2 mm in this time.
32. M. C. Dinauer, T. L. Steck, P. N. Devreotes, *J. Cell Biol.* **86**, 554 (1980).
33. ———, *ibid.*, p. 545.
34. A. Gilman, *Proc. Natl. Acad. Sci. U.S.A.* **67**, 305 (1970).
35. We thank T. L. Steck for use of his laboratory; T. L. Steck, H. S. Tager, M. C. Dinauer, L. M. Keefer, M. D. Lane, P. Englund, M. Lieber, and M. Logan for helpful discussions and critical review of the manuscript; and M. J. Potel and S. A. Mackay for computer graphical analysis of the fluorograph. The original observation of the thin black lines at the distal edge of the movement bands was made by R. L. Clark. This work was supported by PHS grant GM 22321 to T. L. Steck. P.N.D. was a postdoctoral fellow of the Damon Runyon-Walter Winchell Cancer Fund DRG (178F). The work was also supported in part by PHS grants GM 28007 and RR-5378 to P.N.D.
* Address correspondence to P.N.D. Present address: Department of Physiological Chemistry, Johns Hopkins University School of Medicine, Baltimore, Md. 21205.

5 August 1980

Cross-Contamination of Cells in Culture

Abstract. *Lists are presented of references to all known publications describing cell properties that serve to characterize (i) known strains of HeLa and purported human cell lines indicted as HeLa contaminants, (ii) strains of human cell lines contaminated with human but non-HeLa cells, and (iii) strains of cells contaminated by cells from one or more other species. Frequencies of cell cross-contaminations are cited and references are presented to relatively simple techniques that could serve to detect such contamination.*

We present here a comprehensive listing of documented instances of inter- and intraspecies cell culture contamination (Tables 1 to 3) (*1–133*). In 1976 (*26*) we listed the references to all known publications that had served to relate strains of HeLa cells to each other and to indict a large number of other purported human cell lines as HeLa contaminants. A total of 103 sources provided these cultures. Indictment followed when the cells exhibited (i) type A (fast) mobility for G6PD, (ii) type 1 for both PGM1 and PGM3, (iii) absence of a Y chromosome by fluorescent staining, particularly in cases where the cell donors were known to have been male, and (iv) possession of a complex of trypsin-Giemsa banded marker chromosomes reported in known HeLa cells. The list served investigators both as a ready reference to information on HeLa cells and as a signal to the possibility that cells with designations such as those listed might in fact be HeLa cells. The reevaluation of the provenance of published cell lines established from human tumors (*101*) was also of value, because it was among cell lines still extant and available for research that many contaminants were discovered.

When the HeLa cell contamination of many cell lines became known a major effort was made to inform users of cell cultures that in spite of these problems there were available many bona fide lines representing not only the original donors' cells (*102*), but also cells representing the specific tumor of origin (*103*). However, the results of this effort had to be further revised because it was subsequently discovered that while all the cells described were not HeLa, a number of lines had been contaminated with another human tumor cell line, SW-480 (*104*, *105*).

Previously, a number of publications had revealed cell contamination problems, mostly of an interspecies nature, but in general these did not specify the precise contaminating cell line [for summaries see (*106–108*)]. In this report we have tabulated (Table 1) the karyologic, serologic, immunologic, enzymologic, and other data that serve to characterize specific cell cultures. We have updated information on cultures from the same sources as previously listed (*26*) and present references to cultures, many with new designations, from 41 additional sources. The results should serve as an up-to-date reference to contaminated cultures and a further warning that other cultures so designated may be contaminated as well.

Earlier studies concentrated on the mobility patterns of a few isoenzymes (for example, LDH, G6PD, and PGM1 and 2). More recently, cells in culture have been examined for their allozyme genetic signatures representing the composite enzyme phenotype at increasing numbers of loci. The expression of HLA antigens on the cell surface has also been studied more extensively.

In addition to being contaminated with HeLa cells, some human cell lines have been cross-contaminated with other human cells. Detection of type A mobility for G6PD is not in itself sufficient for indictment of a cell as HeLa (*71*, *105*), particularly since there are now a number of newer cell lines expressing this genetic trait (*68*, *71*, *109*). Although this number is still small compared to the number of celis with G6PD type B, it is interesting that a non-HeLa cell with type A may be involved in another contamination event. Thus, one report (*68*) mentions disparity between two cultures of EB-3 cells at different laboratories in regard to G6PD, one being type A, the other type B. EB-3 is a well-known lymphoblast-like cell derived from a patient